OPEN

Reactivation of simian immunodeficiency virus reservoirs in the brain of virally suppressed macaques

Lucio Gama[a], Celina M. Abreu[a,b], Erin N. Shirk[a], Sarah L. Price[a], Ming Li[a], Greg M. Laird[c], Kelly A. Metcalf Pate[a], Stephen W. Wietgrefe[d], Shelby L. O'Connor[e], Luiz Pianowski[f], Ashley T. Haase[d], Carine Van Lint[g], Robert F. Siliciano[c], The LRA-SIV Study Group, Janice E. Clements[a]

See related paper on page 167

Objective: Resting $CD4^+$ T cells have been recognized as the major cell reservoir of latent HIV-1 during antiretroviral therapy (ART). Using an simian immunodeficiency virus (SIV)/macaque model for AIDS and HIV-related neurocognitive disorders we assessed the contribution of the brain to viral latency and reactivation.

Design: Pigtailed macaques were dual inoculated with SIVDeltaB670 and SIV17E-Fr and treated with an efficacious central nervous system-penetrant ART. After 500 days of viral suppression animals were treated with two cycles of latency reversing agents and increases in viral transcripts were examined.

Methods: Longitudinal plasma and cerebrospinal fluid (CSF) viral loads were analyzed by quantitative and digital droplet PCR. After necropsy, viral transcripts in organs were analyzed by PCR, in-situ hybridization, and phylogenetic genotyping based on *env* V1 loop sequences. Markers for neuronal damage and CSF activation were measured by ELISA.

Results: Increases in activation markers and plasma and CSF viral loads were observed in one animal treated with latency reversing agents, despite ongoing ART. SIV transcripts were identified in occipital cortex macrophages by in-situ hybridization and $CD68^+$ staining. The most abundant SIV genotype in CSF was unique and expanded independent from viruses found in the periphery.

Conclusion: The central nervous system harbors latent SIV genomes after long-term viral suppression by ART, indicating that the brain represents a potential viral reservoir and should be seriously considered during AIDS cure strategies.

AIDS 2017, **31**:5–14

Keywords: brain, central nervous system, HIV-1, ingenol-B, latency, latency reversing agents, simian immunodeficiency virus, viral reservoir, vorinostat

[a]Department of Molecular and Comparative Pathobiology, Johns Hopkins School of Medicine, Baltimore, Maryland, USA, [b]Departamento de Genética, Universidade Federal do Rio de Janeiro, Rio de Janeiro, Brazil, [c]Department of Medicine, Johns Hopkins School of Medicine, Baltimore, Maryland, [d]Department of Microbiology and Immunology, University of Minnesota, Minneapolis, [e]Department of Pathology and Laboratory Medicine, University of Wisconsin School of Medicine, Madison, USA, [f]Kyolab, Valinhos, São Paulo, Brazil, and [g]Service of Molecular Virology, Department of Molecular Biology, Université Libre de Bruxelles, Gosselies, Belgium.

Correspondence to Lucio Gama, PhD, Department of Molecular and Comparative Pathobiology, Johns Hopkins School of Medicine, Baltimore, MD, USA.

Tel: +1 410 9559770; fax: +1 410 9559823; e-mail: lucio@jhmi.edu
Received: 25 April 2016; revised: 6 July 2016; accepted: 12 July 2016.

DOI:10.1097/QAD.0000000000001267

Introduction

Despite abundant evidence of HIV-1 infection in the central nervous system (CNS) during the AIDS epidemic [1,2], neuroAIDS is no longer a critical concern in the era of antiretroviral therapy (ART). HIV-1 encephalitis and dementia have declined significantly in patients whose virus replication is well suppressed by ART in peripheral blood. However, there is evidence that 30–50% of HIV-1-infected individuals on long-term ART have mild to moderate HIV-associated neurocognitive disorder (HAND) [3–5] associated with ongoing low-level inflammation in the brain, which can be directly or indirectly related to viral presence in the CNS [6–8]. ART suppresses viral replication and improves survival in HIV-1-infected patients, but does not eliminate replication-competent viral reservoirs [9–11]. Current research on ART intensification and HIV eradication focus on resting $CD4^+$ T cells (rCD4s) with little consideration for the potential of latent reservoirs in other target cells, such as brain macrophages [12,13]. Two patients in an eradication trial in Boston were removed from ART and both developed encephalitis [14], suggesting that viral reservoirs in brain contribute to virus rebound and cause CNS disease. In addition, initial trials of HIV eradication examine only viral load in peripheral blood as an indication of HIV reactivation or change in the latent reservoir, although novel data indicate that many latent HIV-1 genomes are in tissues and may respond differently to latency reversing agents (LRA) [15].

To evaluate the contribution of the brain in virus latency and reactivation during ART we used a well characterized and consistent macaque model for AIDS and HAND in which more than 80% of infected macaques develop simian immunodeficiency virus (SIV)-associated neurological symptoms in 90 days [16]. This model has been previously evaluated under fully suppressed ART and achieved levels of viral suppression similar to those described in ART-treated HIV-1-infected patients [17]. For in-vivo activation of latent reservoirs, we tested a combination of two synergistic LRAs: the protein kinase C (PKC) activator ingenol-B and the histone deacetylase (HDAC) inhibitor vorinostat. Our results show that LRA administration lead to an increase in viral load in cerebrospinal fluid (CSF), indicating that the CNS harbors latent SIV genomes despite long-term ART suppression. Although a small number of animals were assessed, we provide for the first time in-vivo proof of concept that the brain represents a consequential viral reservoir and should be seriously considered during AIDS cure strategies.

Methods

Ethical statements

Macaque studies were approved by the Johns Hopkins University Institutional Animal Care and Use Committee and conducted in accordance with the Weatherall Report, the guide for the care and use of laboratory animals, and animal welfare regulations. Animals were monitored twice daily and given a full physical examination under ketamine sedation at least once every other week throughout the study to monitor for clinical signs of disease. All animals received environmental enrichment and were housed in groups prior to infection. For necropsy, animals were euthanized in accordance with the 2013 American Veterinary Medical Association (AVMA) guidelines for euthanasia of animals using an overdose of sodium pentobarbital under ketamine sedation prior to perfusion with phosphate-buffered saline to remove blood from tissues. Ethical approvals for use of human samples were granted by the Johns Hopkins Institutional Review Board (Baltimore, Maryland, USA) and the Human Subject Ethics Committees of the Saint-Pierre Hospital (Brussels, Belgium). All individuals enrolled in the studies provided written informed consent for donating blood.

Study participants

In the first cohort, ART-treated HIV-1-infected individuals were enrolled in the study at Johns Hopkins Hospital based on the criteria of undetectable plasma HIV-1 RNA level (<50 copies/ml) for a minimum of 6 months. Characteristics of study participants are presented in Table S1, http://links.lww.com/QAD/A981. In a second cohort, HIV-1-infected individuals at the St-Pierre Hospital (Brussels, Belgium) were selected on the basis of the following criteria: volunteers were treated with ART and had undetectable plasma HIV-1 RNA levels (20 copies/ml) for at least one year, and had a level of $CD4^+$ T lymphocytes higher than 300 cells/μl of blood. Characteristics of patients are presented in Table S2, http://links.lww.com/QAD/A981.

Ex-vivo measurement of intracellular HIV-1 mRNA induction from resting $CD4^+$ T cells (leukapheresis)

Peripheral blood mononuclear cells (PBMCs) from whole blood or continuous-flow centrifugation leukapheresis product were purified using density centrifugation on a Ficoll-Hypaque gradient. rCD4s were enriched by negative depletion as described [11,18]. Cells were cultured in RPMI 10% fetal bovine serum (FBS) at a concentration of 5×10^6 cells/ml. Intracellular HIV-1 mRNA was measured as described previously [11,18]. Briefly, rCD4s isolated from HIV-1-infected individuals on suppressive ART were treated with each compound for 18 h. The following concentrations were used: 0.2% dimethyl sulfoxide, 10 nmol/l ingenol-B, 50 ng/ml PMA plus 1 μmol/l ionomycin. Total RNA was isolated, and RT-qPCR was performed. Serial dilutions of a plasmid containing the last 352 nucleotides of viral RNA plus 30 deoxyadenosines were used for a molecular standard curve (pVQA; available from NIH AIDS Reagent program, # 12666).

Latency model in CD8$^+$-depleted peripheral blood mononuclear cells

CD8$^+$-depleted PBMCs were isolated from blood of HIV-1-infected patients as previously described [19,20]. One day after isolation, cells were mock treated, treated with 10 nmol/l ingenol-B or anti-CD3/anti-CD28 antibodies as a positive control. Six days after treatment, culture supernatants were collected for RNA extraction. HIV-1 RNA levels were quantified using the Generic HIV RNA kit (Biocentric, Bandol, France) according to manufacturer's instructions. Total cellular DNA was extracted from CD8$^+$-depleted PBMCs and viral DNA was then quantified by ultrasensitive qPCR (Generic HIV DNA cell kit; Biocentric [21]) according to manufacturer's instructions.

Animal studies

Five juvenile pigtailed macaques (*Macaca nemestrina*) were inoculated intravenously. with SIV/Delta B670 and SIV/17E-Fr, as previously described [22]. Animals started ART at 12 days p.i. Three animals (Mn0, Mn1, and Mn2) were suppressed for 503 days and then used for LRA-induced viral reactivation experiments. Two macaques (Mn3 and Mn4) were suppressed for 200 days and then removed from ART for viral rebound studies. Details on the macaque studies can be found in the supplemental material, http://links.lww.com/QAD/A981.

In-vitro latency model in macaque

rCD4s were isolated from PBMCs using magnetic beads. CD4$^+$ T-cells were first isolated using the CD4$^+$ T cell isolation kit for nonhuman primates (Stemcell Technologies, Vancouver, Canada), according to the manufacturer. For the depletion of activated CD4$^+$ T cells, a second incubation with antibodies anti-CD25, anti-CD69, and anti-human leukocyte antigen - antigen D-related (HLA-DR) was performed, obtaining 85–95% pure cell populations. Three million rCD4s were plated in RPMI 10% FBS with 5 μmol/l zidovudine and treated with 100 nmol/l ingenol-B, 50 ng/ml PMA plus 1 μmol/l ionomycin, or kept as untreated control. After 18 h, cells were harvested and RNA was isolated for SIV *gag* quantification by reverse transcription quantitative polymerase chain reaction (RT-qPCR), as described below.

Quantification of simian immunodeficiency virus virions in plasma and central nervous system and simian immunodeficiency virus RNA in tissues and peripheral blood mononuclear cells

Virus was quantitated from 140 μl of plasma or CSF collected longitudinally. Viral RNA was isolated using the QIAamp Viral RNA Mini kit (Qiagen, Valencia, California, USA), according to the manufacturer's protocol. For viral RNA in tissues, total RNA was isolated from 50 mg of tissues or 10^7 PBMCs using the RNeasy kit (Qiagen), and treated with two units of Turbo DNase (Life Technologies) for 30 min at 37°C. Quantification of virion-associated RNA was performed by RT-qPCR using the QuantiTect Virus kit (Qiagen) and a primer/probe set for SIV *gag*: SIV21F: 5′-GTCTGCGTCATCTGGTGCATTC-3′, SIV22R: 5′-CACTAGGTGTCTCTGCACTATCTGTTTTG-3′, and SIV23: FAM-5′-CTTCCTCAGTGTGTTTCACTTTCTCTTCTG-3′-BH1 (Integrated DNA Technologies, Coralville, Iowa, USA). Reactions were performed in a Roto-Gene Q thermocycler (Qiagen) with the following cycles: 50°C/30 min, 95°C/10 min, and 45 cycles of 95°C/15 s, 55°C/15 s, and 60°C/30 s. For the quantitation of SIV RNA in tissues, digital droplet PCR (ddPCR) was performed in a Bio-Rad QX-100 system as previously described [23], using the same primer/probe set used for the detection of SIV *gag* by qPCR.

Quantification of activation markers and neuronal damage in cerebrospinal fluid

ELISA kits were used to measure levels of CCL2 (R&D), neopterin, and neurofilament light chain (IBL International) in CSF, according to manufacturers' protocols.

In-situ hybridization

In total 8-mm thick sections from fresh frozen, optimum cutting temperature (OCT)-embedded brain tissue samples were processed as previously described [24]. After acetylation and dehydration, samples were hybridized at 45°C overnight with a 35S-labeled riboprobe and 0.5 mmol/l aurintricarboxylic acid in hybridization mix. Riboprobes were synthesized from 1 kb templates amplified from SIVDeltaB670 cDNA by PCR. After ribonuclease treatment, tissue sections were dehydrated, coated in Kodak NTB emulsion, exposed at 4°C for 7–14 days, and developed and fixed per manufacturer's instructions. Slides were stained with hematoxylin and mounted with Permount. Section areas for each digitally acquired picture were obtained using an Aperio CS2 scanner (Leica, Wetzlar, Germany). Section weights were estimated from their 8-μm thickness and their area. For fluorescent in-situ hybridization (ISH) combined with immunofluorescence, 6-mm thick sections of formalin fixed paraffin embedded tissues were hybridized with a SIVDeltaB670 RNAscope probe (Advanced Cell Diagnostics, Newark, New Jersey, USA) after they had been processed as per manufacturer's directions. Signal was amplified with a fluorescent multiplex kit and detected with Atto 550. Sections were incubated with mouse anti-CD68 (Dako, Carpinteria, California, USA) overnight at 4°C, detected with antimouse IgG Alexa 488 (Invitrogen, Carlsbad, California, USA), and mounted with Aquapolymount (Polysciences, Warrington, Pennsylvania, USA). Photographic images for both ISHs were taken with an Olympus DP72 camera on an Olympus BX60 microscope.

RNAseq for the phylogenic analysis of *Env* V1 region

Env V1 region amplicons from plasma and CSF SIV RNA and tissue SIV DNA were generated by PCR using nested primers as previously described [25]. Amplicons

were tagged using the TruSeq DNA PCR free HT kit (Illumina, San Diego, California, USA). Successfully tagged products were purified with AmPure XP beads (Beckman Coulter, Brea, California, USA), quantified, and pooled. Approximately 14 pm of pooled DNA was then loaded onto a 600-cycle MiSeq Reagent Kit V3 on an Illumina MiSeq. FASTQ reads were then imported into Geneious V 7.1.7 (Biomatters, Ltd, Auckland, New Zealand). Reads were trimmed, paired, and merged using fast length adjustment of short reads (FLASH). Merged reads were mapped back to a consensus sequence generated from a stock of this virus. Reads spanning the amplicon of interest were extracted, and only those of sizes 450–500 bp were considered. Identical duplicates were detected and frequencies were calculated. For the phylogenetic analysis, reads were mapped to the reference sequence for the V1 portion of SIV/DeltaB670 *env*, using Geneious V 8.1.7. After de-novo assembling, contiguous reads were quantitated and extracted for analysis. Results are presented as nucleotide or amino acid sequence alignment assessed by ClustalW and phylogenetic UPGMA trees using Neighbor-joining consensus genetic distance model.

Results

We have previously established a reproducible and accelerated SIV macaque model for AIDS and HAND [16,26]. The model was also used to successfully demonstrate the efficacy of ART in suppressing SIV and in decreasing the number of infected rCD4s to levels similar to those in ART-treated HIV-1 infected individuals [17,22,26]. To rigorously develop an ART suppression model to evaluate latent reservoirs in the brain that closely resembles long-term treatment in virally suppressed patients, three SIV-infected macaques started receiving a CNS-penetrant ART regimen (tenofovir, darunavir, ritonavir, and the integrase inhibitor L-870812) [27] at 12 days post inoculation (p.i.). After 400 days of viral suppression, defined as fewer than 30 SIV copies/ml in plasma measured by qPCR and confirmed by digital droplet PCR, one animal (Mn0) was maintained as procedural control and two macaques (Mn1 and Mn2) were treated with latency reversing agents. Because no Food and Drug Administration-approved compound has been successfully used to reactivate HIV-1 latent reservoirs in virally suppressed humans or nonhuman primates [28–31], we used the novel PKC activator ingenol-B, which had been previously evaluated *in vitro* and was efficient in activating HIV-1 long-term repeats in reporter cell lines [32–34]. Before testing the compound in our SIV-macaque model, however, we evaluated whether ingenol-B activates viral genomes in ex-vivo primary cells. We initially tested the LRA in two distinct HIV-1 latency models with successful results (Fig. 1a and b). Then, to corroborate the HIV-1 data, we evaluated ingenol-B *ex vivo* in rCD4s isolated from SIV-infected macaques that have been virally suppressed for more than 180 days, which is the minimum time in humans for blood rCD4 viral reservoirs to stabilize [35]. Similarly to what was observed in the HIV-1 models, the compound significantly increased viral transcription, demonstrating that ingenol-B also activates SIV in macaque latently infected rCD4s (Fig. 1c). Based on these results, and also on previous studies done on dogs, it shows that the compound can be administered orally to mammals for more than 14 days without causing apparent side-effects (Fig. S1, http://links.lww.com/QAD/A981), we started the in-vivo experiments using our SIV macaque model [17,36].

For the first round of ingenol-B treatment, we chose to administer 0.4 mg/kg per day, which is 10% of the nonobserved adverse effect level established in toxicology studies (Fig. S1, http://links.lww.com/QAD/A981). After 30 days of treatment we did not observe increase in plasma viral load and therefore treated the animals for

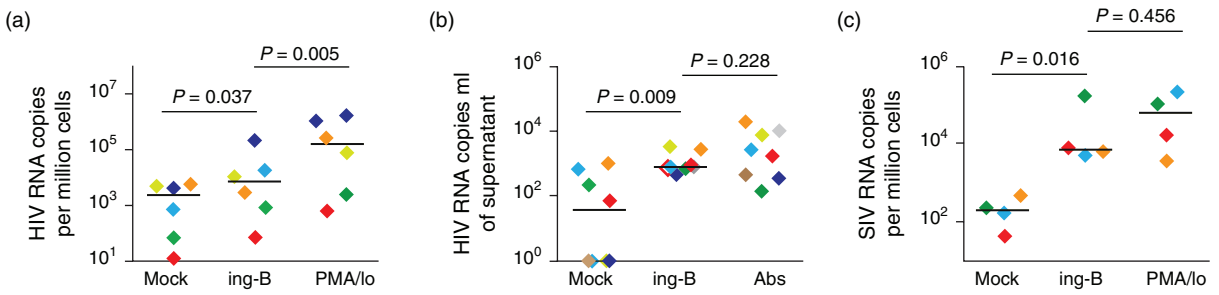

Fig. 1. Ingenol-B regulates viral expression in three distinct latency models from different cohorts. For each set, paired samples are represented by the same color. (a) rCD4s isolated from HIV-infected-ART-treated patients at the Johns Hopkins hospital (Table S1, http://links.lww.com/QAD/A981) were incubated in ingenol-B, using PMA/Ionomycin as positive control. (b) $CD8^+$-depleted PBMCs isolated at the University of Brussels from virally suppressed patients (Table S2, http://links.lww.com/QAD/A981) were treated with ingenol-B. Activation with anti-CD3/CD28 antibodies was used as positive control. Viral production in supernatant was quantitated by qPCR. (c) rCD4s from SIVdeltaB670/SIV17E-Fr-infected ART-treated macaques were incubated with ingenol-B, using PMA/Ionomycin as positive control.

10 more days with an increased dose of 0.6 mg/kg per day. Again, no changes in viral load were observed and ingenol-B treatment was withdrawn for 2 weeks. Treatment was reinitiated and maintained for 10 days at 1 mg/kg per day in combination with the HDAC inhibitor vorinostat (6 mg/kg subcutaneous infusion four times), which is known to synergize with PKC agonists and does not appear to successfully impact viral reservoirs as monotherapy [18,37]. Animals were kept on CNS-penetrant ART until the end of the experiment and suppressive levels of antiretroviral drugs were detected in blood, brain, spleen, and liver of all three macaques (Table S3, http://links.lww.com/QAD/A981). By the end of the dual-LRA treatment, macaque Mn2 showed detectable plasma viral load, which increased for several days after LRAs were withdrawn (Fig. 2a). No change in viral load was observed in the other LRA-treated animal Mn1 or the untreated Mn0.

The increase of plasma viral load in macaque Mn2 was concomitant with an increase of SIV viral RNA in CSF (Fig. 2b). In addition, we observed a simultaneous increase in CNS immune activation markers (CCL2 and neopterin) and in the neuronal damage marker neurofilament light chain [38], which began before the cotreatment with vorinostat (Fig. 2c). CSF viral load was 10 times higher than plasma despite the CNS-penetrant suppressive ART and the animal was euthanized 18 days after LRA interruption because of neurological symptoms (lethargy and lack of appetite).

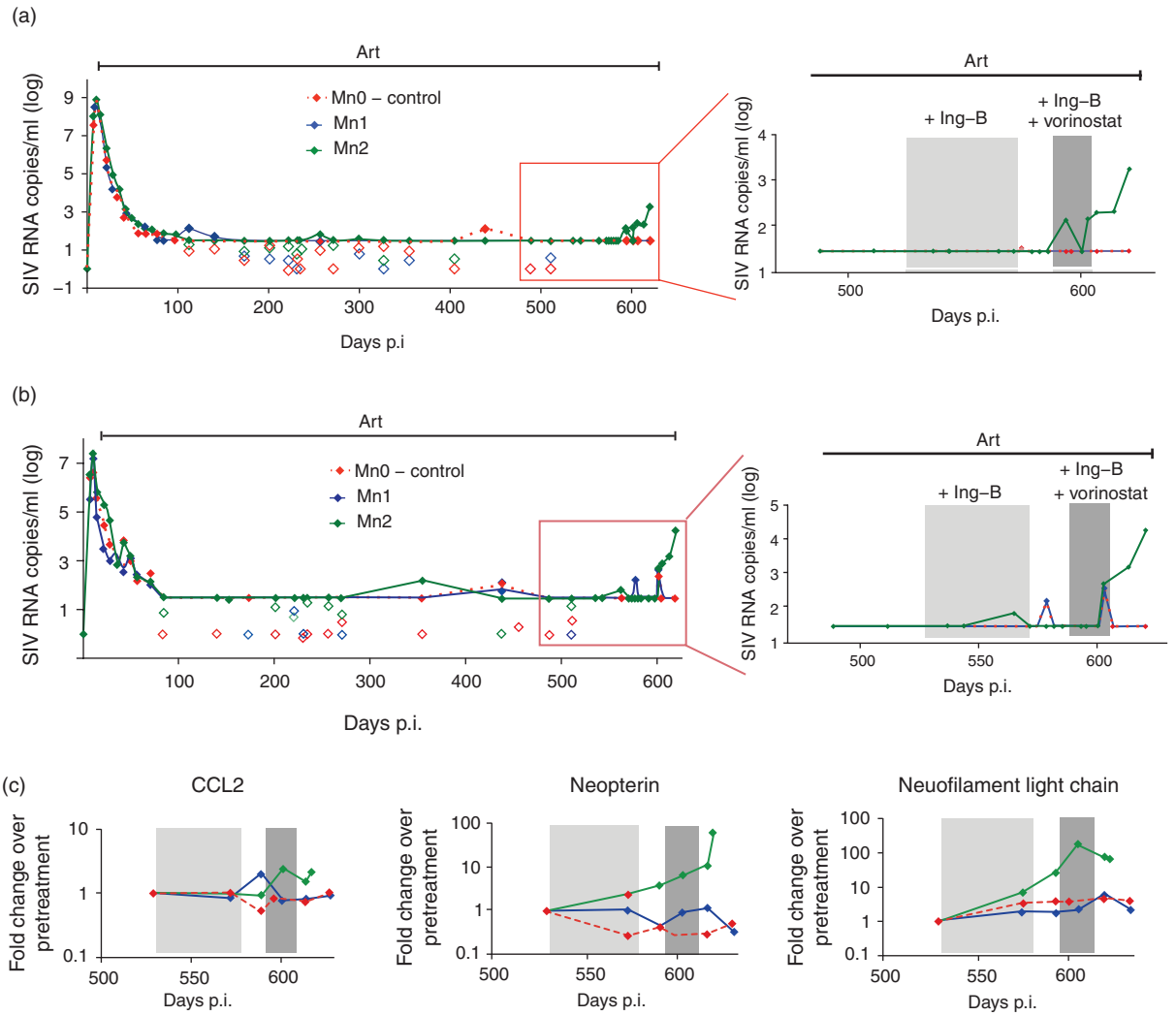

Fig. 2. Treatment with latency reversing agents increases plasma and cerebrospinal fluid viral load and activation markers in SIV-infected pigtailed macaques virally suppressed for 400 days. Three SIV-infected pigtailed macaques were ART-treated starting at 12 days p.i. Macaque Mn0 (red) was kept as control whereas macaques Mn1 (blue) and Mn2 (green) were treated with ingenol-B starting at 530 days p.i. Time of treatment with ingenol-B is marked in light gray, and with ingenol-B plus vorinostat in dark gray. Plasma (a) and cerebrospinal fluid (b) viral loads were measured by qPCR (lines) and, in some points, confirmed by ddPCR (hollow diamonds). (c) Changes in the cerebrospinal fluid levels of CCL2, neopterin, and neurofilament light chain measured by ELISA.

Table 1. Levels of SIV RNA isolated from organs of macaques Mn0, Mn1, and Mn2, quantitated by digital droplet PCR.

	SIV RNA copies/μg RNA		
	Mn0	Mn1	Mn2
Occipital cortex	3	<1	1700
Basal ganglia	3	2	3
Parietal cortex	4	<1	19
Axilary LN	3	7	10
Bronchial LN	4	10	7
Colonic LN	15	17	50
Retropharyngeal LN	6	3	NA
Submandibular LN	7	5	14
Spleen	18	120	124
Liver	15	359	3
Lung	5	12	4
Kidney	84	5	16
Ileum	<1	<1	<1
Jejunum	<1	<1	12
Colon	<1	<1	<1

LN, lymph node.

To assess the origin of the virus detected in CSF, postmortem RNA samples from different brain regions were analyzed by ddPCR. A significant level of SIV RNA was observed in the occipital cortex of Mn2 (1700 copies/μg RNA) when compared with Mn0 and Mn1 (3 and < 1 copies/μg RNA, respectively; Table 1). These values, however, were considerably lower than RNA levels historically observed in our model in brain of animals with symptoms associated with SIV encephalitis [22]. Viral reactivation appeared to be focal as SIV RNA levels in other parts of brain (basal ganglia and parietal cortex) were as low as those in the LRA untreated animal. ISH results corroborated the PCR findings showing focal, that is,. individual cells expressing viral RNA in occipital cortex parenchyma, in and near microglial nodules (Fig. 3a, Table S4, http://links.lww.com/QAD/A981). No SIV RNA was detected by ISH in other brain regions. SIV RNA colocalized with $CD68^+$ cells, indicating infection and reactivation in brain macrophages (Fig. 3b). To compare LRA-induced viral reactivation to viral recrudescence after ART withdrawal, we analyzed brain tissue of two virally suppressed macaques (Mn3 and Mn4, Fig. S2, http://links.lww.com/QAD/A981) who were euthanized when plasma viral load was first detectable after cessation of ART (3–4 days). Although macaque Mn3 showed lower levels of SIV RNA in brain and CSF when compared with Mn2 (164 versus 1700copies/μg brain RNA and 149 versus 18 000copies/ml of CSF), a greater number of clustered foci with varied intensities were observed in its occipital cortex (Fig. 3a), suggesting viral spread. In the LRA-untreated macaque Mn0, the LRA-treated macaque Mn1, and ART-withdrawn macaque Mn4, brain tissues were negative for SIV RNA by ISH and ddPCR.

Genotypic analyses done on the V1 region in *Env* of SIV RNA in plasma and CSF by RNA sequencing demonstrated that the most abundant variant in CSF (Mn2-Seq5) in macaque Mn2 was unique and had only 81.9–83.3% homology to those in the plasma (Fig. 4a–d). This suggests that LRA treatment activated distinct genomes that persisted in the CNS compartment despite long-term viral suppression. In the ART-withdrawn macaques Mn3 and Mn4, in which viral reactivation was LRA-independent, sequences from both plasma and CSF were indistinguishable from DNA sequences found in PBMCs (Fig. 4e). In contrast, in LRA-treated Mn2 macaque, the Mn2-Seq5 variant was unique to the CSF

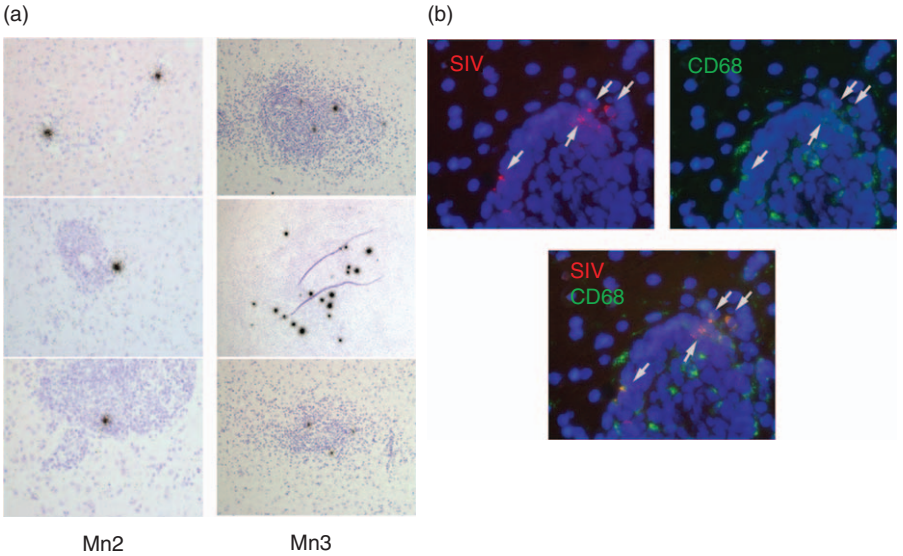

Fig. 3. In-situ hybridization detects SIV RNA in the occipital cortex of macaques Mn2 (treated with ART and LRA) and Mn3 (treated with and then released from ART). (a) ISH shows focal distribution of SIV RNA+in macaque Mn2 and clustered positive cells in macaque Mn3. 40× magnification. (b) Colocalization of SIV RNA (ISH-red) and CD68 (IHC-green) in macaque Mn2. 60× magnification. Arrows shows positive staining for each marker.

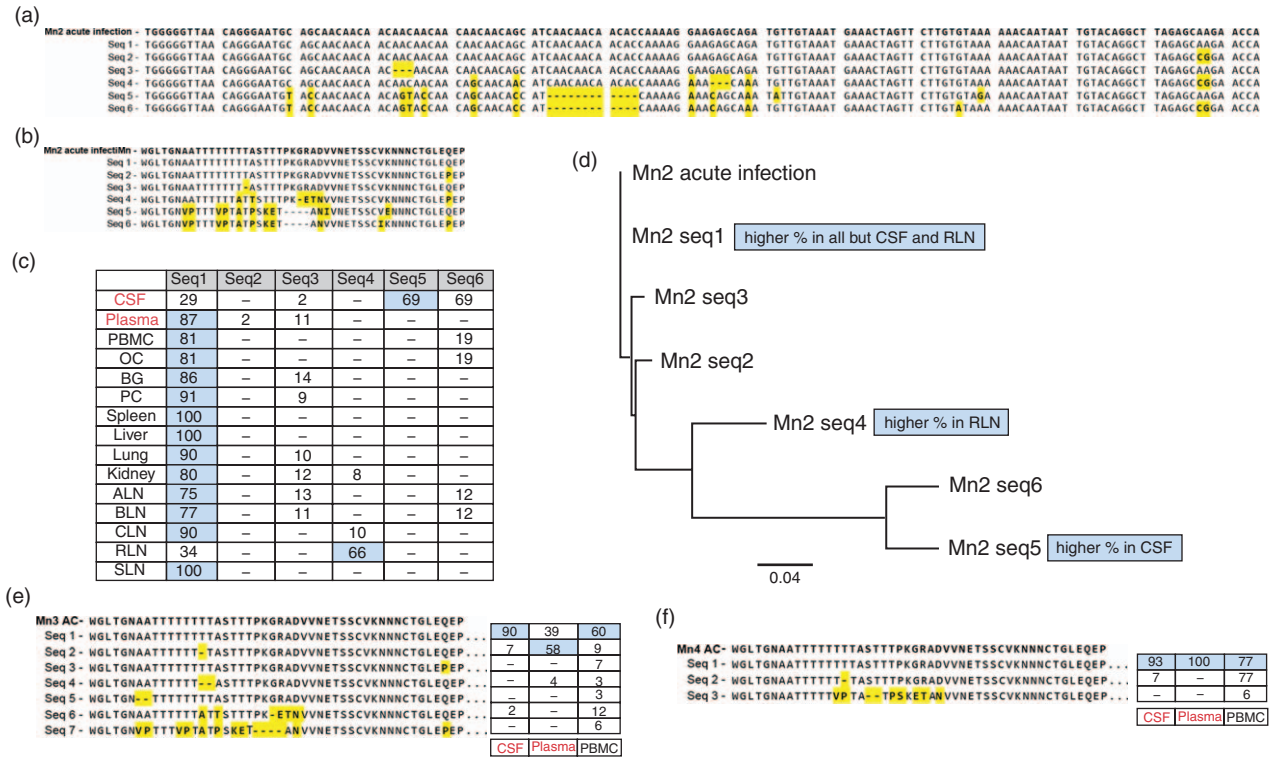

	Seq1	Seq2	Seq3	Seq4	Seq5	Seq6
CSF	29	–	2	–	69	69
Plasma	87	2	11	–	–	–
PBMC	81	–	–	–	–	19
OC	81	–	–	–	–	19
BG	86	–	14	–	–	–
PC	91	–	9	–	–	–
Spleen	100	–	–	–	–	–
Liver	100	–	–	–	–	–
Lung	90	–	10	–	–	–
Kidney	80	–	12	8	–	–
ALN	75	–	13	–	–	12
BLN	77	–	11	–	–	12
CLN	90	–	–	10	–	–
RLN	34	–	–	66	–	–
SLN	100	–	–	–	–	–

	CSF	Plasma	PBMC
Seq 1	90	39	60
Seq 2	7	58	9
Seq 3	–	–	7
Seq 4	–	4	3
Seq 5	–	–	3
Seq 6	2	–	12
Seq 7	–	–	6

	CSF	Plasma	PBMC
Seq 1	93	100	77
Seq 2	7	–	77
Seq 3	–	–	6

Fig. 4. Unique SIV variant is found in the cerebrospinal fluid of macaque Mn2. (a) *Env* V1 region sequences identified in RNA isolated from plasma and cerebrospinal fluid and DNA isolated from tissues of macaque Mn2 at terminal time point. Yellow highlights deletions or mutations, compared with the most abundant DNA sequence found in PBMCs at acute infection (ac-14 days p.i). (b) Translated amino acid sequences from the nucleotides in (a). (c–d) Analysis of nucleotide sequences from Mn2; table (c) showing their prevalence (%), with blue highlighting the most abundant sequence for each compartment and phylogenetic tree (d). (e–f) Phylogenetic analyses of SIV RNA (plasma and cerebrospinal fluid) and DNA (PBMC) *Env* V1 region amino acid sequences isolated from macaques Mn3 (e) and Mn4 (f) at terminal time point, after release from ART. Tables on the right show their prevalence (in percentage), with blue highlighting the most abundant sequence for each compartment. OC, occipital cortex; BG, basal ganglia; PC, parietal cortex; ALN, axillary lymph node; BLN, bronchial lymph node; CLN, colonic lymph node; RLN, retropharyngeal lymph node; SLN, submandibular lymph node.

and was not represented in viral DNA samples isolated from PBMCs and peripheral tissues at necropsy.

Discussion

Before the advent of ART, cognitive impairment caused by HIV-1 affected up to 50% of patients [39], indicating that, at that time, at least half of HIV-1-infected patients harbored viral genomes in the brain. In this era of efficacious ART, similar number of patients is affected by neurologic dysfunctions, the majority of which are milder forms. In addition, some groups have reported the presence of viral RNA in the CSF of treated patients [40]. Our macaque model for AIDS and HAND has been successfully used as an ART model as well, with full viral suppression in both periphery and CNS [17,26]. Here we demonstrate that, after 400 days of suppression, LRA treatment reactivated latent virus that could be detected in plasma and tissues, including brain. Reactivation in peripheral tissues and CNS occurred independently, as demonstrated by distinct SIV genotypes isolated from each compartment. Lack of cell-to-cell viral spread in the brain during LRA induction suggests that the observed levels of antiretroviral drugs in the CNS were effective and prevented *de novo* viral replication. The increasing levels of viral RNA in the CSF after LRA interruption appeared to be unrelated to viral spread, as indicated by the focal reactivation observed in brain by ISH. In contrast, two macaques released from suppressive ART demonstrated cell-to-cell viral spread in brain parenchyma and genotypically identical SIV genotypes in CSF and plasma. In addition, the identification of at least four distinct circulating SIV genotypes substantiates the LRA-activation hypothesis over the possibility of the development of ART-resistant strains. Yet, regardless of whether viral increase in CSF was directly caused by LRA activation, we demonstrate that macrophages in brain harbor replicative competent SIV after long-term ART treatment. Longitudinal surveillance of CSF showed an increase in viral load concomitant with detectable plasma viremia during the dual LRA induction. Inflammatory

markers in this animal were upregulated in CSF by the end of the first ingenol-B cycle, prior to the addition of vorinostat, suggesting that immune activation in the CNS occurred independently of the HDAC inhibitor. Further, viral RNA in CSF was 10-fold greater than in plasma and presented unique phenotypically distinct genotypes that were not present in the periphery. Because of the focal nature of SIV infection [16], extensive sampling of brain sections would be necessary to precisely determine the CNS origin of Mn2-Seq5. These results suggest that LRA treatment in one of the macaques led to compartmentalized activation in the CNS, which may represent an obstacle for a complete and well tolerated viral eradication in HIV^+ patients.

Other organs apart from brain showed increase in viral RNA expression after LRA treatment. Current reports point to follicular helper T cells as the major $CD4^+$ T-cell compartment for HIV-1 infection and latent reservoirs [41]. A potential mechanism for the effect of LRA treatment is that the compounds reactivated latently infected follicular T cells, triggering increase in leukocyte trafficking into lymphoid tissues. Specifically, in one of the macaques, significant viral reactivation was observed in the liver, an organ that is not commonly associated with HIV-1 reservoirs.

Thus, our data suggest that the presence of virus-producing genomes in the CNS should be a cause of concern during AIDS cure strategies aimed at reactivating latent viral genomes. Increased immune activation in the brain, as we observed, may lead to reactivation of latent reservoirs followed by an exacerbated and harmful inflammatory response even in the presence of ART. As the CNS harbors macrophages with persistent replication-competent virus, monitoring CSF for viral activation or residual viremia should be seriously considered during eradication strategies.

Acknowledgements

The authors thank Gilead, Merck, Bristol-Myers Squibb, Abbvie, Janssen, and Amazônia Fitomedicamentos Ltda for providing the antiretrovirals and LRAs. We thank Dr Angela Kashuba (University of North Carolina) for antiretroviral mass spectrometry analysis.

L.G.: Conceived the project, analyzed data, organized and wrote the manuscript; Celina M. Abreu: Conceived some of the experiments, analyzed data, helped with the manuscript; Erin N. Shirk: Responsible for all cytometry data; Sarah L. Price: Performed and analyzed the *ex vivo* macaque model for SIV latency; M.L.: Responsible for all qPCR and ddPCR data; Greg M. Laird: Performed and analyzed the Johns Hopkins model for HIV latency; Kelly A Metcalf Pate: Designed the animal protocol, supervised veterinary activities, analyzed *in vivo* data; Stephen W. Wietgrefe: Performed and analyzed the ISH data; Shelby L. O'Connor: Analyzed the phylogenetic data; L.P.: Designed the compound ingenol-B and tested it in dogs; Ashley T. Haase: Analyzed the ISH data; C.V.L.: Conceived some of the experiments, analyzed the ULB model for HIV latency; Robert F. Siliciano: Conceived some of the experiments, analyzed the Johns Hopkins model for HIV latency, helped with the manuscript; Janice E. Clements: Conceived the project, analyzed data, helped with the manuscript.

The LRA-SIV Study Group – S.E.Q.: Responsible for all ELISA measurements and analyses; B.T.B.: Responsible for the collection and preparation of all longitudinal samples (blood, CSF); J.C.: Responsible for RNA and DNA isolation from macaque tissues; L.F.P.F.: Analyzed all toxicology data in dogs; D.G: Responsible for all RNAseq data; S.E.B.: Responsible for the clinical pathology analysis of all animals; L.M.M.: Responsible for the clinical evaluation of all animals; R.J.A.: Veterinarian responsible for the animal model, helped designing the animal protocol.

K.P.: Performed the dual staining for ISH and IHC; C.R.: Performed all PCR from the ULB model for HIV latency; S.D.E.W: Selected patients and collected samples for the ULB model; A.K.: Performed some of the experiments for the ULB model for HIV latency; G.D.: Performed some of the experiments for the ULB model for HIV latency; C.Z.: Advised on the animal study, helped with the manuscript; J.L.M.: Advised on the animal study, helped with the manuscript.

The LRA-SIV Study Group: Suzanne E Queen (Department of Molecular and Comparative Pathobiology, Johns Hopkins School of Medicine, Baltimore, MD), Brandon T Bullock (Department of Molecular and Comparative Pathobiology, Johns Hopkins School of Medicine, Baltimore, MD), Josh Croteau (Department of Molecular and Comparative Pathobiology, Johns Hopkins School of Medicine, Baltimore, MD), Luiz F Pianowski Filho (Department of Microbiology and Immunology, University of Minnesota, Minneapolis, MN), Dane Gellerup (Department of Pathology and Laboratory Medicine, University of Wisconsin School of Medicine, Madison, WI), Sarah E Beck (Department of Molecular and Comparative Pathobiology, Johns Hopkins School of Medicine, Baltimore, MD), Lisa M Mangus (Department of Molecular and Comparative Pathobiology, Johns Hopkins School of Medicine, Baltimore, MD), Robert J Adams (Department of Molecular and Comparative Pathobiology, Johns Hopkins School of Medicine, Baltimore, MD), Katherine Perkey (Kyolab, Valinhos SP 13273, Brazil), Christine Rouzioux (Service of Molecular Virology, Department of Molecular Biology (DBM), Université Libre de Bruxelles, Gosselies CP 300, Belgium), Stéphane de Wit (Necker Hospital, Paris, France), Anna Kula (Saint-Pierre Hospital, Brussels, Belgium), Gilles

Darcis (Saint-Pierre Hospital, Brussels, Belgium), Chris Zink (Department of Molecular and Comparative Pathobiology, Johns Hopkins School of Medicine, Baltimore, MD), Joseph L Mankowski (Department of Molecular and Comparative Pathobiology, Johns Hopkins School of Medicine, Baltimore, MD).

Research reported in this publication was supported by NIH grants P01MH070306–01, U19A1076113, and P40OD013117. It was also supported in part by the Office of the Director, NIH under Award Number P51OD011106 to the WNPRC, UW-Madison. This research was conducted in part at a facility constructed with support from Research Facilities Improvement Program grant numbers RR15459–01 and RR020141–01. Work in C.V.L.'s lab was supported by the ANRS (France Recherche Nord&Sud Sida-HIV Hépatites), the Belgian Fund for Scientific Research (FRS-FNRS Belgium), the ''Fondation Roi Baudouin, the NEAT program, and the Wallo on Region (the Excellence Program Cibles). A.K. is a postdoctoral fellow of 'Les Amis des Instituts Pasteur à Bruxelles, asbl'.

Conflicts of interest

There are no conflicts of interest.

References

1. Epstein LG, Sharer LR, Cho ES, Myenhofer M, Navia B, Price RW. **HTLV-III/LAV-like retrovirus particles in the brains of patients with AIDS encephalopathy.** *AIDS Res* 1984; **1**:447–454.
2. Gyorkey F, Melnick JL, Sinkovics JG, Gyorkey P. **Retrovirus resembling HTLV in macrophages of patients with AIDS.** *Lancet* 1985; **1**:106.
3. Ances BM, Clifford DB. **HIV-associated neurocognitive disorders and the impact of combination antiretroviral therapies.** *Curr Neurol Neurosci Rep* 2008; **8**:455–461.
4. Heaton RK, Clifford DB, Franklin DR Jr, Woods SP, Ake C, Vaida F, *et al*. **HIV-associated neurocognitive disorders persist in the era of potent antiretroviral therapy: CHARTER Study.** *Neurology* 2010; **75**:2087–2096.
5. Heaton RK, Franklin DR, Ellis RJ, McCutchan JA, Letendre SL, Leblanc S, *et al*. **HIV-associated neurocognitive disorders before and during the era of combination antiretroviral therapy: differences in rates, nature, and predictors.** *J Neurovirol* 2011; **17**:3–16.
6. Eden A, Fuchs D, Hagberg L, Nilsson S, Spudich S, Svennerholm B, *et al*. **HIV-1 viral escape in cerebrospinal fluid of subjects on suppressive antiretroviral treatment.** *J Infect Dis* 2010; **202**:1819–1825.
7. Yilmaz A, Yiannoutsos CT, Fuchs D, Price RW, Crozier K, Hagberg L, *et al*. **Cerebrospinal fluid neopterin decay characteristics after initiation of antiretroviral therapy.** *J Neuroinflammation* 2013; **10**:62.
8. Spudich S, Gonzalez-Scarano F. **HIV-1-related central nervous system disease: current issues in pathogenesis, diagnosis, and treatment.** *Cold Spring Harb Perspect Med* 2012; **2**:a007120.
9. Finzi D, Blankson J, Siliciano JD, Margolick JB, Chadwick K, Pierson T, *et al*. **Latent infection of CD4+ T cells provides a mechanism for lifelong persistence of HIV-1, even in patients on effective combination therapy.** *Nat Med* 1999; **5**:512–517.
10. Chomont N, El-Far M, Ancuta P, Trautmann L, Procopio FA, Yassine-Diab B, *et al*. **HIV reservoir size and persistence are driven by T cell survival and homeostatic proliferation.** *Nat Med* 2009; **15**:893–900.
11. Bullen CK, Laird GM, Durand CM, Siliciano JD, Siliciano RF. **New ex vivo approaches distinguish effective and ineffective single agents for reversing HIV-1 latency in vivo.** *Nat Med* 2014; **20**:425–429.
12. Siliciano JD, Siliciano RF. **Recent developments in the search for a cure for HIV-1 infection: targeting the latent reservoir for HIV-1.** *J Allergy Clin Immunol* 2014; **134**:12–19.
13. Honeycutt JB, Wahl A, Baker C, Spagnuolo RA, Foster J, Zakharova O, *et al*. **Macrophages sustain HIV replication in vivo independently of T cells.** *J Clin Invest* 2016; **126**:1353–1366.
14. Henrich TJ, Hu Z, Li JZ, Sciaranghella G, Busch MP, Keating SM, *et al*. **Long-term reduction in peripheral blood HIV type 1 reservoirs following reduced-intensity conditioning allogeneic stem cell transplantation.** *J Infect Dis* 2013; **207**:1694–1702.
15. Lorenzo-Redondo R, Fryer HR, Bedford T, Kim EY, Archer J, Kosakovsky Pond SL, *et al*. **Persistent HIV-1 replication maintains the tissue reservoir during therapy.** *Nature* 2016; **530**:51–56.
16. Clements JE, Mankowski JL, Gama L, Zink MC. **The accelerated simian immunodeficiency virus macaque model of human immunodeficiency virus-associated neurological disease: from mechanism to treatment.** *J Neurovirol* 2008; **14**:309–317.
17. Dinoso JB, Rabi SA, Blankson JN, Gama L, Mankowski JL, Siliciano RF, *et al*. **A simian immunodeficiency virus-infected macaque model to study viral reservoirs that persist during highly active antiretroviral therapy.** *J Virol* 2009; **83**:9247–9257.
18. Laird GM, Bullen CK, Rosenbloom DI, Martin AR, Hill AL, Durand CM, *et al*. **Ex vivo analysis identifies effective HIV-1 latency-reversing drug combinations.** *J Clin Invest* 2015; **125**:1901–1912.
19. Bouchat S, Gatot JS, Kabeya K, Cardona C, Colin L, Herbein G, *et al*. **Histone methyltransferase inhibitors induce HIV-1 recovery in resting CD4(+) T cells from HIV-1-infected HAART-treated patients.** *AIDS* 2012; **26**:1473–1482.
20. Reuse S, Calao M, Kabeya K, Guiguen A, Gatot JS, Quivy V, *et al*. **Synergistic activation of HIV-1 expression by deacetylase inhibitors and prostratin: implications for treatment of latent infection.** *PLoS One* 2009; **4**:e6093.
21. Avettand-Fenoel V, Chaix ML, Blanche S, Burgard M, Floch C, Toure K, *et al*. **LTR real-time PCR for HIV-1 DNA quantitation in blood cells for early diagnosis in infants born to seropositive mothers treated in HAART area (ANRS CO 01).** *J Med Virol* 2009; **81**:217–223.
22. Zink MC, Brice AK, Kelly KM, Queen SE, Gama L, Li M, *et al*. **Simian immunodeficiency virus-infected macaques treated with highly active antiretroviral therapy have reduced central nervous system viral replication and inflammation but persistence of viral DNA.** *J Infect Dis* 2010; **202**:161–170.
23. Strain MC, Lada SM, Luong T, Rought SE, Gianella S, Terry VH, *et al*. **Highly precise measurement of HIV DNA by droplet digital PCR.** *PLoS One* 2013; **8**:e55943.
24. Zeng M, Smith AJ, Wietgrefe SW, Southern PJ, Schacker TW, Reilly CS, *et al*. **Cumulative mechanisms of lymphoid tissue fibrosis and T cell depletion in HIV-1 and SIV infections.** *J Clin Invest* 2011; **121**:998–1008.
25. Babas T, Vieler E, Hauer DA, Adams RJ, Tarwater PM, Fox K, *et al*. **Pathogenesis of SIV pneumonia: selective replication of viral genotypes in the lung.** *Virology* 2001; **287**:371–381.
26. Clements JE, Gama L, Graham DR, Mankowski JL, Zink MC. **A simian immunodeficiency virus macaque model of highly active antiretroviral treatment: viral latency in the periphery and the central nervous system.** *Curr Opin HIV AIDS* 2011; **6**:37–42.
27. Letendre S, Marquie-Beck J, Capparelli E, Best B, Clifford D, Collier AC, *et al*. **Validation of the CNS penetration-effectiveness rank for quantifying antiretroviral penetration into the central nervous system.** *Arch Neurol* 2008; **65**:65–70.
28. Shang HT, Ding JW, Yu SY, Wu T, Zhang QL, Liang FJ. **Progress and challenges in the use of latent HIV-1 reactivating agents.** *Acta Pharmacol Sin* 2015; **36**:908–916.
29. White CH, Johnston HE, Moesker B, Manousopoulou A, Margolis DM, Richman DD, *et al*. **Mixed effects of suberoylanilide hydroxamic acid (SAHA) on the host transcriptome and proteome and their implications for HIV reactivation from latency.** *Antiviral Res* 2015; **123**:78–85.
30. Badia R, Grau J, Riveira-Munoz E, Ballana E, Giannini G, Este JA. **The thioacetate-omega(gamma-lactam carboxamide) HDAC inhibitor ST7612AA1 as HIV-1 latency reactivation agent.** *Antiviral Res* 2015; **123**:62–69.

31. Miana GA, Riaz M, Shahzad-Ul-Hussan S, Paracha RZ, Paracha UZ. **Prostratin: an overview.** *Mini Rev Med Chem* 2015; **15**:1122–1130.
32. Abreu CM, Price SL, Shirk EN, Cunha RD, Pianowski LF, Clements JE, *et al*. **Dual role of novel ingenol derivatives from Euphorbia tirucalli in HIV replication: inhibition of de novo infection and activation of viral LTR.** *PLoS One* 2014; **9**:e97257.
33. Pandelo Jose D, Bartholomeeusen K, da Cunha RD, Abreu CM, Glinski J, da Costa TB, *et al*. **Reactivation of latent HIV-1 by new semi-synthetic ingenol esters.** *Virology* 2014; **462-463**:328–339.
34. Jiang G, Mendes EA, Kaiser P, Sankaran-Walters S, Tang Y, Weber MG, *et al*. **Reactivation of HIV latency by a newly modified ingenol derivative via protein kinase Cdelta-NF-kappaB signaling.** *AIDS* 2014; **28**:1555–1566.
35. Blankson JN, Finzi D, Pierson TC, Sabundayo BP, Chadwick K, Margolick JB, *et al*. **Biphasic decay of latently infected CD4+ T cells in acute human immunodeficiency virus type 1 infection.** *J Infect Dis* 2000; **182**:1636–1642.
36. Zink MC, Clements JE. **A novel simian immunodeficiency virus model that provides insight into mechanisms of human immunodeficiency virus central nervous system disease.** *J Neurovirol* 2002; **8 (Suppl 2)**:42–48.
37. Ling B, Piatak M Jr, Rogers L, Johnson AM, Russell-Lodrigue K, Hazuda DJ, *et al*. **Effects of treatment with suppressive combination antiretroviral drug therapy and the histone deacetylase inhibitor suberoylanilide hydroxamic acid; (SAHA) on SIV-infected Chinese rhesus macaques.** *PLoS One* 2014; **9**:e102795.
38. Beck SE, Queen SE, Witwer KW, Metcalf Pate KA, Mangus LM, Gama L, *et al*. **Paving the path to HIV neurotherapy: predicting SIV CNS disease.** *Eur J Pharmacol* 2015; **759**:303–312.
39. Grant I, Atkinson JH, Hesselink JR, Kennedy CJ, Richman DD, Spector SA, *et al*. **Evidence for early central nervous system involvement in the acquired immunodeficiency syndrome (AIDS) and other human immunodeficiency virus (HIV) infections. Studies with neuropsychologic testing and magnetic resonance imaging.** *Ann Intern Med* 1987; **107**:828–836.
40. Ellis RJ, Moore DJ, Childers ME, Letendre S, McCutchan JA, Wolfson T, *et al*. **Progression to neuropsychological impairment in human immunodeficiency virus infection predicted by elevated cerebrospinal fluid levels of human immunodeficiency virus RNA.** *Arch Neurol* 2002; **59**:923–928.
41. Perreau M, Savoye AL, De Crignis E, Corpataux JM, Cubas R, Haddad EK, *et al*. **Follicular helper T cells serve as the major CD4 T cell compartment for HIV-1 infection, replication, and production.** *J Exp Med* 2013; **210**:143–156.